PART III

Spatial Analysis and Statistical Modeling of Infectious Diseases

CHAPTER 8

Analyzing the Potential Impact of Bird Migration on the Global Spread of H5N1 Avian Influenza (2007–2011) Using Spatiotemporal Mapping Methods

Heather Richardson and Dongmei Chen
Department of Geography, Faculty of Arts and Science, Queen's University, Kingston, ON, Canada

8.1 INTRODUCTION

H5N1 is a type of influenza virus that causes a highly infectious and severe respiratory disease in birds named avian influenza (or "bird flu") and occasionally in humans (Gilbert et al. 2006). A greater understanding of the mechanisms of H5N1 spread is necessary due to the severity of the influenza as a threat to human health. After its initial outbreaks in domestic poultry and wild bird populations, it crossed the species barrier in 1997 and has begun infecting humans (Wallace et al. 2007). Though human-to-human infection has been rare, the human mortality rate of H5N1 is high. The World Health Organization has reported a total of 549 cases (58.3% mortality rate) of human infections over 15 countries between 2003 and 2011.

Several measures exist in order to control the disease: restricting animal movement, quarantine, disinfection, culling, stamping out, and vaccination. Wallace et al. (2007) has reported that hundreds of millions of domestic and migratory birds have been killed by H5N1 or culled in an effort at control. Despite these efforts, intermittent and sporadic outbreaks in poultry continue to be reported worldwide (Capu and

Analyzing and Modeling Spatial and Temporal Dynamics of Infectious Diseases, First Edition.
Edited by Dongmei Chen, Bernard Moulin, and Jianhong Wu.

Au: Please check sh[illegible] RH OK

Alexander 2010). Previously, waterfowl seemed exempt from the widespread infection since only sporadic cases were reported; however, as of 2005 there have been many more infections of waterfowl beginning in western China (Liu et al. 2005). The occurrence of highly pathogenic H5N1 infection of waterfowl indicates that the virus has the potential to be a global threat since the lake of origin is a breeding ground for migrant birds (Liu et al. 2005). Evidently, the virus is rapidly crossing spatial and biological boundaries. Given the virus's precipitous spread, the control of H5N1 is currently one of the highest priorities in global health.

Significant research has been conducted on the past spread of H5N1 in order to predict the virus's movement. Kilpatrick et al. (2006) made several key findings regarding the pathways by which the virus has and will spread as of 2006. It was concluded that the spread of H5N1 in Asia and Africa included introductions both by poultry and wild birds, whereas the spread to European countries was more consistent with the movements of wild birds (Kilpatrick et al. 2006). As of 2006, the highest risk of H5N1 introduction to the Americas is through the trade in poultry, not from migratory birds ~~(Kilpatrick et al. 2006)~~. Due to the synergy between poultry and migratory bird pathways, countries adjacent to poultry importers, including the United States, are at higher risk for H5N1 introduction ~~(Kilpatrick et al. 2006)~~.It was also found that the synergistic spread was first by poultry in Southeast Asia and then by migratory birds into Europe ~~(Kilpatrick et al. 2006)~~. Also, infectious bird days are associated with wild bird migration after cold weather events in Eastern Europe ~~(Kilpatrick et al. 2006)~~. After reviewing the findings of Kilpatrick et al. (2006), it should be considered that surveillance for H5N1 introduction in wild birds should focus on finding and testing sick and dead (rather than live) birds arriving from the south and the north and that outbreaks were inconsistent with reported trade, implying possible unreported or illegal trade or the migration of birds that was not discovered until later.

In a previous study, Zhang et al. (2012) had investigated the spatiotemporal dynamics of global H5N1 outbreaks between December 2003 and December 2009. These characteristics can offer clues that may enhance understanding ~~of the dynamics~~ of disease spread~~. This understanding~~ allow~~s~~ the identification of targeted areas where investigations are needed. The insights of spatiotemporal dynamics are relevant because they may enhance the cost-effectiveness of planning and the implementation of disease-control measures (Oyana et al. 2006). In a study in southern China in 2004, it was found that the directional finding was very consistent with the major migratory bird routes in East Asia; however, due to the poor surveillance and reporting systems in the regions, it was concluded that the study's findings warranted further evaluation (Oyana et al. 2006). Zhang et al. (20[illegible]) ~~found that the start date of the epidemic was postponed, the duration of the epidemic was prolonged, and its magnitude reduced over time, but the disease transmission cycle was not fully interrupted~~.

Distinct spatial patterns in poultry and wild birds exist. These differences suggest that there are also different environmental drivers and potentially different spread mechanisms (Si et al. 2013). In Si et al.'s study (2013), wild bird outbreaks were strongly associated with an increased Normalized Difference Vegetation Index (NDVI) and lower elevation but were similarly affected by climatic conditions as

compared with poultry outbreaks. Outbreaks in poultry were most prevalent where the location of farms or trade areas overlapped with habitats for wild birds (Si et al. 2013). On the other hand, outbreaks in wild birds were mainly found in areas where food and shelters were available (Si et al. 2013). These different environmental drivers propose that different spread mechanisms may exist. Most likely, HPAI H5N1 spread to poultry via both poultry and wild birds, whereas contact with wild birds alone seems to drive the outbreaks in wild birds (Si et al. 2013).

Several methods have been used to map the spread of influenza based on known outbreak points. This step is critical for understanding the spread mechanisms of influenza and to facilitate the administration of mitigation and prediction techniques later; therefore, there is a need for innovative mapping techniques over a larger temporal and spatial (global) scale. Saito et al. (2005) used the Kriging method to map influenza activity in Europe. While this method showed a potential for mapping in Europe over the 2004–2005 seasons, it is only applicable over a small temporal and spatial scale since they only created difference values between the two major peaks of the season. Given the geometry of the continents, especially when considering outbreak spread to countries separated by oceans, as well as the various migration pathways a bird may follow, this method is too simplistic for a global analysis of H5N1.

In another study by Skog et al. (2008), the author studied how the Russian influenza in Sweden in 1889–1890 was disseminated to all other places by creating Thiessen (or Voronoi) polygons around each of the 69 studied locations of the observation points (outbreaks) where cases had been reported. The principle was that all positions within a polygon are closer to the point location, around which the polygon was created, than to any other of the remaining 68 location points. Similar to the methods used by Saito et al. (2005), they proved useful for a small-scale study depending on human-to-human transfer; however, the methods would not be appropriate for H5N1 spread via bird migration because the influenza can be transferred over long distances within a small period of time. Furthermore, they assumed that influenza spread in the same way in all regions; however, this assumption would be inappropriate when studying the spread of H5N1, which transfers among local clusters directly but also by migration or trade. Also, their results offer a general directionality but not discrete pathways.

The goal of this study is to examine the global mechanisms of H5N1 spread during 2007–2011 and determine if global trading and bird migration processes still play similar roles as in the past. To accomplish this objective, an initial analysis included the identification of trends and distribution of outbreaks in order to identify hotspots and epidemic waves (EWs). The Spatial Radial Distance Query Tool (SRDQT) was then implemented to find the temporal difference of start dates and distance between each pair of outbreaks. Finally, the spatiotemporal characteristics of the outbreaks were used to place each outbreak into a cluster. These clusters were joined chronologically by polylines, the lines that exceeded the thresholds were deleted, and the remaining lines were compared with the known migration routes established by Kilpatrick et al. (2006). ~~This paper will~~ outline these methods in their entirety and discuss the results and conclusions of the spatiotemporal analysis.

8.2 METHODOLOGY

8.2.1 Data

Global HPAI H5N1 outbreak data from 2006 to 2011 was collected online from the World Organisation of Animal Health (OIE) and the Food and Agriculture Organization of the United Nations (FAO). The global country boundary map was obtained from the website of Global Administrative Areas. Similar processes to those in Zhang et al. (2010) were used to integrate them into one dataset based on the administrative units of subdistrict. Each outbreak was geocoded to the centroids of outbreak subdistricts with its given coordinates.

Au: Please check if the edits made in the sentence "First, daily epidemic distributions..." are OK

8.2.2 Methods of Analysis

First, daily epidemic distributions of global HPAI H5N1 outbreaks from 2006 to 2011 were constructed to show the magnitude of outbreaks and temporal trends for each continent. As in the study by Zhang et al. (2012), outbreaks were defined as "the confirmed presence of disease, clinically expressed or not, in at least one individual in a defined location and during a specified period of time" (Toma et al. 1999).

Next, the spatial outbreaks were mapped monthly to search the seasonal and spatial outbreak patterns including areas where the virus had been newly introduced, the concentration of outbreaks per country per year, and to identify various spatial "hotspots" and four EWs throughout the study period (2007–2011). During an EW, the number of disease outbreaks peaked rapidly and then decreased gradually until the epidemic was over (Zhang et al. 2010).

In order to evaluate the potential causes of H5N1 spread, the spatial distance and time intervals between outbreaks were calculated using the spatial-time distance query tool named SRDQT, developed at the Laboratory of Geographic Information and Spatial Analysis. (X_i, Y_i, T_i) represent the X, Y coordinates and the starting date of the outbreak i, while (X_i, Y_i, T_j) represents the X, Y coordinates and the starting date of the outbreak j. In this tool, the time difference $(T_i - T_j)$ between start dates and the distance (sqrt$((X_i - X_j)^2 + (Y_i - Y_j)^2)$ between outbreaks i and j are calculated. All outbreak pairs during each EW from 2006 to 2011 were initially calculated without any temporal or spatial filters.

The time intervals and space distances between the start dates of two adjacent outbreaks represent the estimated spreading time and distance of the virus, and are used to indicate the potential causes of the spreading. For instance, if the virus has spread a large distance over too short a time period, migration can be ruled out as the method of spread.

The spatial and temporal intervals were sorted to filter out results over the maximum temporal and rate cutoffs. The maximum time difference cutoff was defined as 7 days. The World Health Organization indicates the H5N1 incubation period to range between 2 and 8 days and possibly as long as 17 days; the organization suggests "that an incubation period of seven days be used for field investigations and the monitoring of patient contacts" (World Health Organization 2013). Though the rate

of bird migration is quite variable, the maximum flight rate cutoff was defined as 725 km per day based on the report from The Kentucky Department of Fish and Wildlife Resources that ducks and geese, the species most commonly associated with avian influenza viruses (AIVs), might travel as much as 727 km a day (USGS 2013). This cutoff was used to classify points that may have spread by migration versus trade or been entirely separate events. With these thresholds in place, spatiotemporal analyses were run again, this time observing only the pairs that may have been transmitted through migration.

In order to identify how local the "clusters" of outbreaks were in the four EWs, each outbreak and its 20 closest neighbors were searched. The distance and day difference between start dates of each outbreak and its 20 closest neighbours were then calculated. The "Nearest Neighbour" function in ArcGIS was used to calculate the average nearest neighbor distances and its clustering significances.

Based on the spatiotemporal characteristics of the virus spread that were determined from the above methods, each outbreak was given a "Cluster ID." The centroid of each cluster was mapped and, using the "XYToLine" tool in ArcGIS, the central points were connected in order to visualize the spread of the virus over time. These lines were compared with the migration route lines mapped by Kilpatrick et al. (2006) to evaluate how dependent the spread was on bird migration.

8.3 RESULTS AND DISCUSSION

Figure 8.1 shows the time series of daily H5N1 outbreaks from 2007 to 2011 globally and by each affected continent (Asia, Africa, and Europe). Four additional EWs were identified over the period of 2007–2011. First, EW1 began in October 2007, peaked in January 2008, and ended in October 2008; EW2 peaked in January 2009 and ended in October 2009; EW3 peaked in February 2010 and ended in September 2010; lastly, EW4 peaked in February 2011. From Figure 8.1, it is clear that the majority of global H5N1 outbreaks came from Asia, the trend of global series corresponds closely with the trend of Asia.

There have remained no introductions into North America as of December 2011 and no new introductions into Europe between January 2007 and December 2011 (Table 8.1). In Europe, there were no outbreaks in 2009 or 2011 and only seven since 2007. Using the description of species for each outbreak in the report as an indicator, there have been several introductions into Southeast Asia as a result of poultry.

By taking note of annual peaks in outbreak occurrence, some aspects of the dynamic of disease spread can be determined. To achieve this, the outbreak starting months were mapped in Figure 8.2.

Zhang et al. (2012) identified two "hotspot" regions of H5N1 outbreaks in well-documented locations in East and Southeast Asia as well as at a novel location at the boundary of Europe and Africa during December 2003 to December 2009. Since then, there has not been a reappearance of outbreaks at the boundary between Europe and Africa; however, hotspots in East and Southeast Asia have remained consistent. During the December 2003 to December 2010 period, outbreaks of H5N1

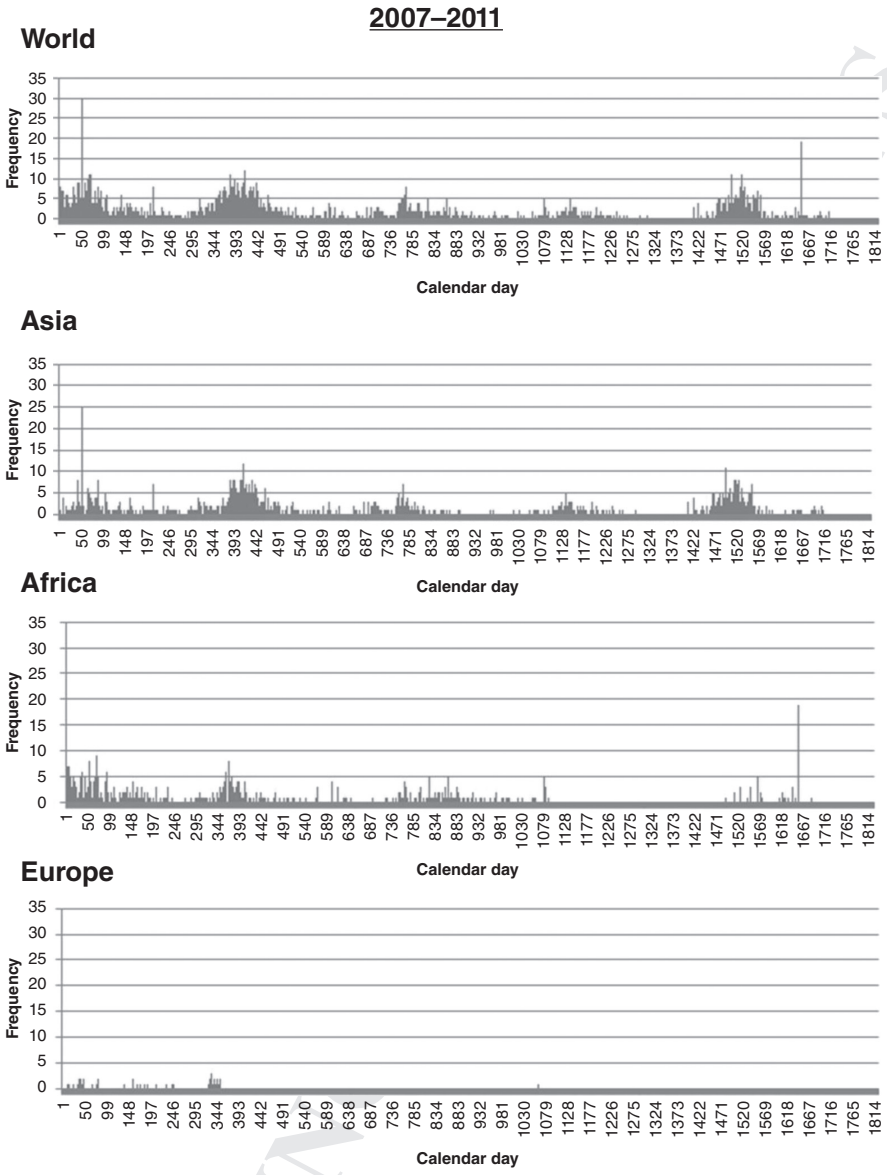

Figure 8.1 Daily epidemic curves of H5N1 outbreak starting days from 2007 to 2011 by continent. Frequency of outbreaks is plotted versus 365 calendar days

Table 8.1 Summary of All Total Outbreaks and Introductions into New Countries from 2007 to 2011

	2007	2008	2009	2010	2011
Outbreaks/year	721	578	243	110	515
H5N1 introductions into new countries (month of initial outbreak; method of spread)	Bangladesh (February; poultry) Saudi Arabia (March; poultry) China (March; poultry) Togo (June; wild then poultry	N/A	Nepal (January; wild)	Bhutan (February; poultry)	Palestine (February; poultry) South Africa (February; poultry)

were common in winter and early spring, which suggests these are higher risk periods (Zhang et al. 2012). Likewise, our analysis from 2007 until 2011 shows there is a high frequency of outbreaks from October to March (Figure 8.2). Interestingly, there are also brief peaks in frequency in Asia during June 2007 and in Africa during June 2011. Based on the distance and time difference between outbreak pairs, the rate between distance and time intervals were calculated to give clues about the method of spread. After applying the 7 day and 725 km per day filters to the SRDQT query results, the distribution of rate (distance/time (km per day)) was found. The rate (~~distance between pairs (km) per days between pairs)~~ at the first quartile was approximately 38, 25, 26, 24, and 27 for outbreak pairs in EW1, EW2, EW3, EW4, and all outbreaks, respectively. In general, frequency declined rapidly as the rate increased and leveled out around 75 km per day where there is no longer any indication of clustering around outbreak centers. During EW1, there was a greater occurrence of outbreaks within a small spatial scale.

The rate of distance and time between each outbreak and its 20 closest neighbors were shown in Figure 8.3 in order to identify how local the "clusters" of outbreaks were distributed in each EW. Considering the high distances, though less frequent, for many of the low neighbor levels there are several isolated outbreaks. Interestingly, the distribution of distance is tiered for EW4 between neighbor levels 6 and 20, and seems to have the most low distance values compared with the other EWs. The average nearest neighbor distance (Table 8.2) shows that EW4 had the most local outbreaks compared with the other EWs. Since the nearest neighbor ratio is less than one, the pattern of outbreak locations within all EWs exhibit clustering (Table 8.2). EW4 has the greatest clustering, followed by EW1, EW2, and EW3 (Table 8.2).

To visualize spread of the influenza over time, the centroids of the clusters were connected chronologically with polylines to create "cluster paths" (Figure 8.4). Since the outbreaks were grouped using the spatial and temporal filters, all outbreaks within one cluster may have been an influence of bird migration. All of the "cluster paths" larger than 5075 km represent low or no risk of spreading H5N1 via bird migration

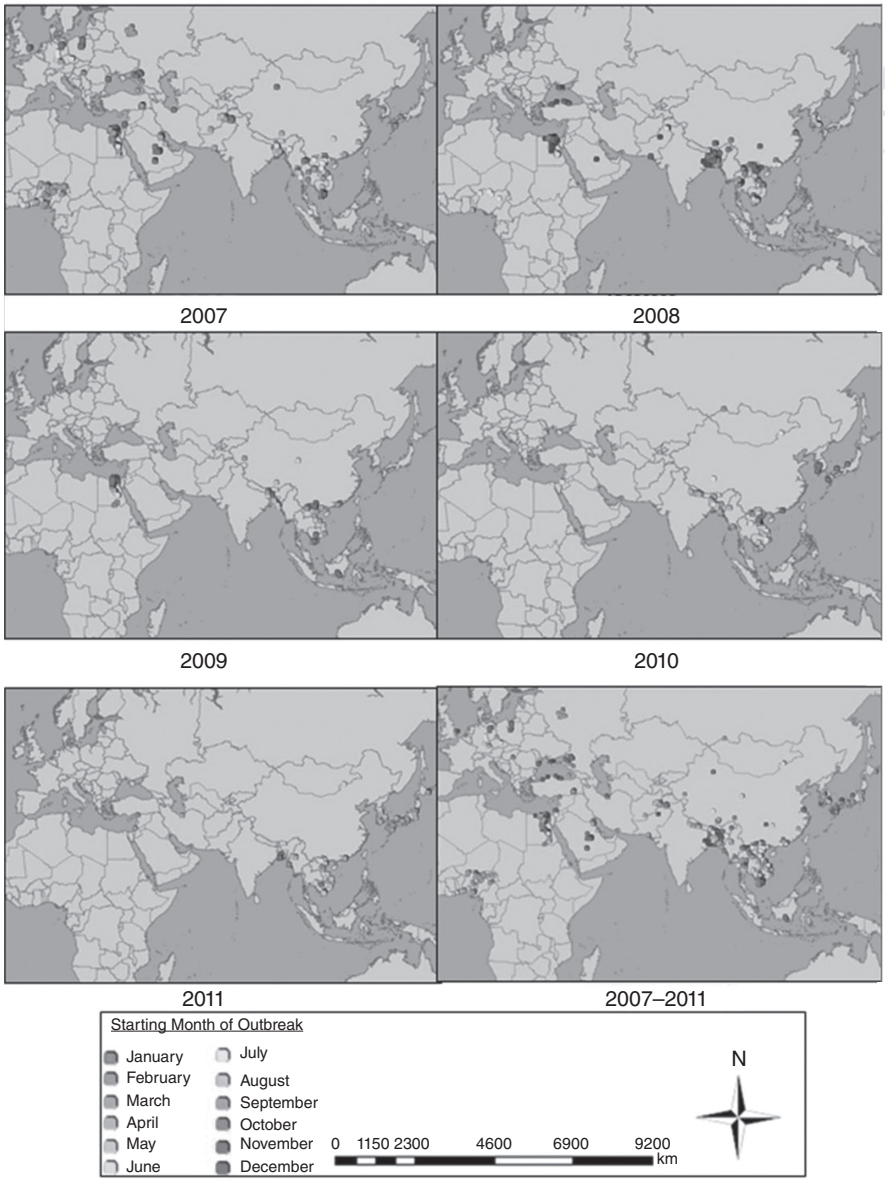

Figure 8.2 Starting month of H5N1outbreaks by year (2007– 201

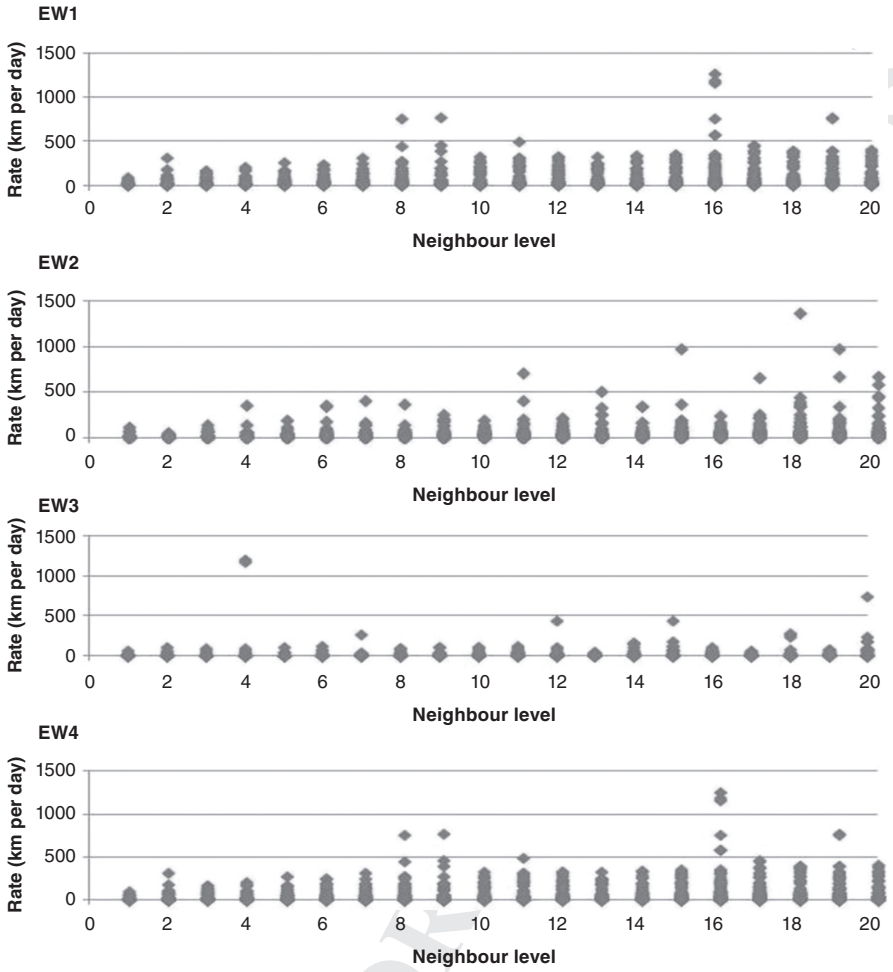

Figure 8.3 Rate (distance/time (km per day)) between each outbreak and its 20 closest neighbours.

Table 8.2 Average Nearest Neighbor Distance in Each Epidemic Wave

	EW1	EW2	EW3	EW4
Observed mean distance (km)	19.23	20.06	22.10	13.30
Expected mean distance (km)	13.63	128.58	147.63	176.75
Nearest neighbor ratio	0.14	0.16	0.15	0.07
z-score:	−39.5	−42.2	−27.4	−39.64
p-value:	0	0	0	0

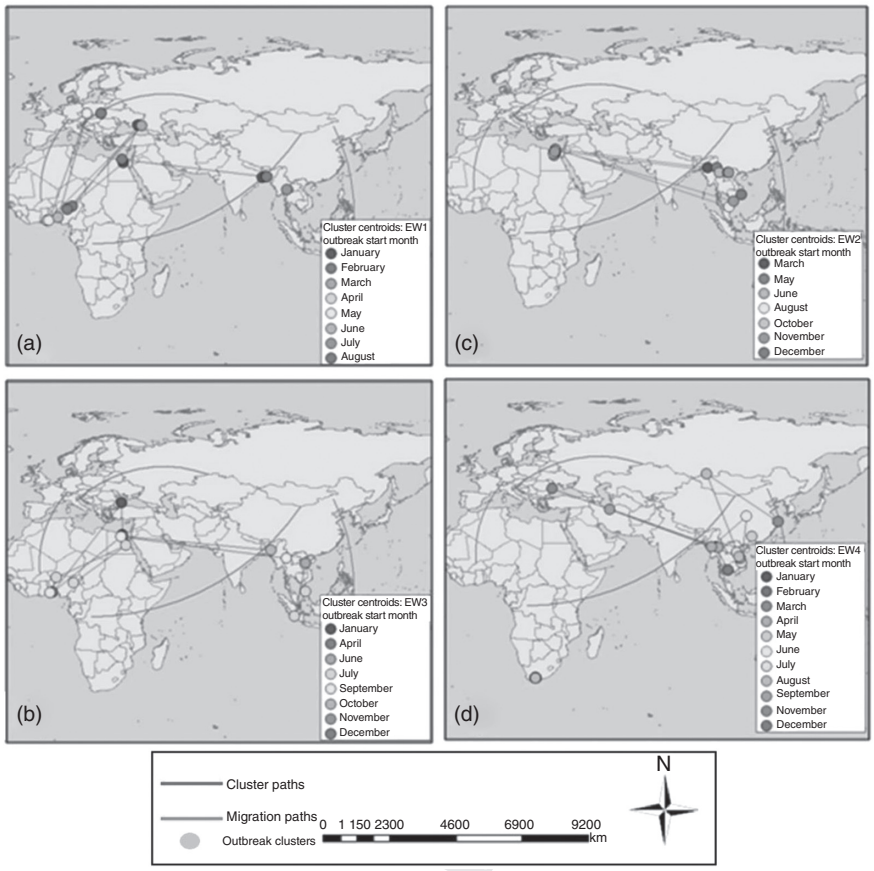

Figure 8.4 Mapping potential pathways of H5N1 spread by comparing cluster paths and known migration paths

and were deleted since this distance exceeds the 7 day limit, assuming the bird flies no faster than 725 km per day. "Cluster paths" smaller than 5075 km and along similar routes as the known migration paths, represent possible mechanisms of H5N1 spread via bird migration. With these conditions in mind, it seems plausible that bird migration may facilitate spread between Africa and Europe during EW1, throughout central Europe, and throughout Southeast Asia during all EWs. Also, isolated clusters represent outbreaks that were not likely facilitated by bird migration. By cross-referencing back to the "Method of Spread" maps presented earlier, these outbreaks can be eliminated as potential pathways for spread via bird migration. For instance, the cluster at the top of South Africa in EW3 is isolated from the potential migration pathways and is identified as spreading by wild bird movement rather than poultry trade (Figure 8.4).

Using the species type and number of cases listed for each outbreak, the method of spread was determined for 2007–2011 and compared with Kilpatrick's results (Figure 8.5). Kilpatrick et al. (2006) estimated that numbers of H5N1 infectious

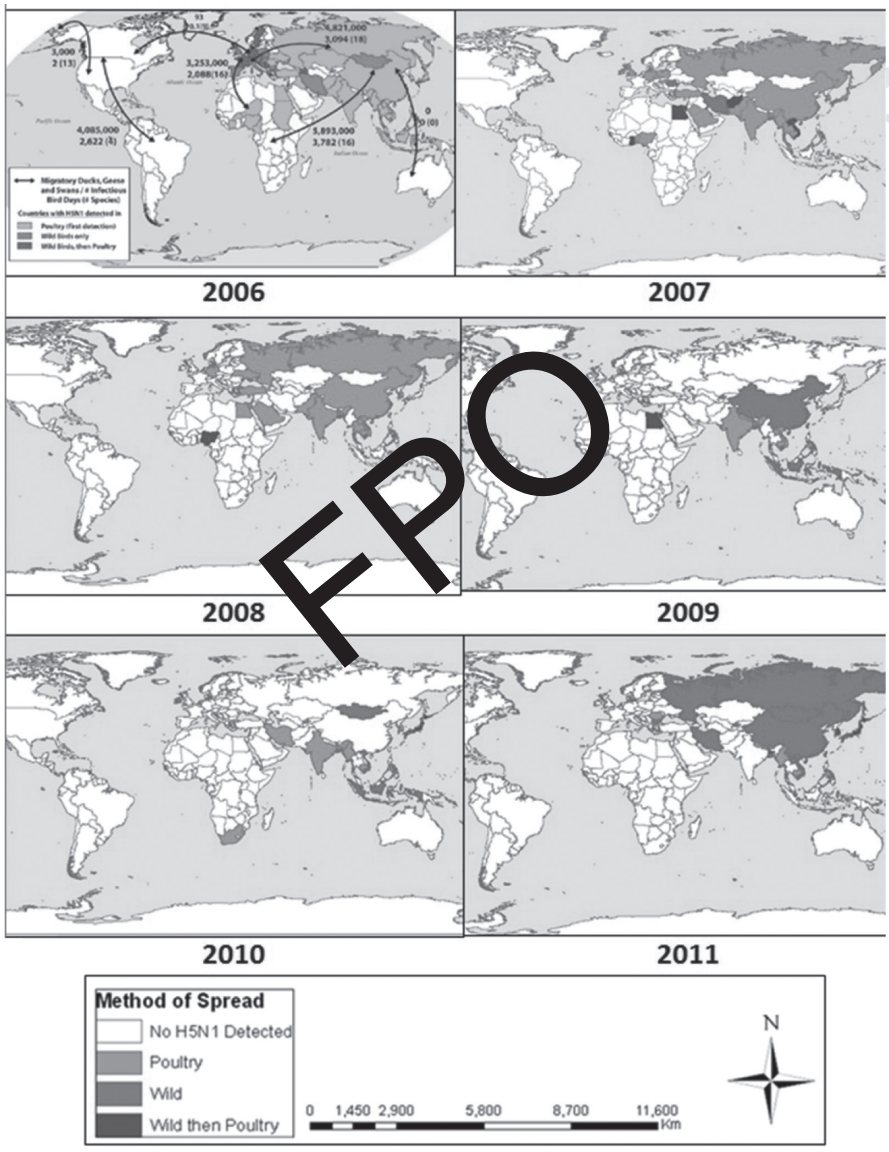

Figure 8.5 Annual comparison of countries with H5N1 detected in (a) poultry (first detected), (b) wild birds only, and (c) wild birds then poultry. Map of 2006 (top left) from Kilpatrick et al. (2006)

bird days associated with poultry trade were more than 100-fold higher than for the other two pathways (wild bird trade and migratory birds) for introductions into Indonesia, Vietnam, Cambodia, Laos, Malaysia, Kazakhstan, Azerbaijan, Iraq, and Cote D'Ivoire and 57-fold higher for Sudan. Oppositely, the number of infectious bird days was >58-fold higher for migrating birds passing first through regions with H5N1 and then to Thailand, Croatia, Ukraine, Niger, Bosnia and Herzegovina, Slovakia, Switzerland, Serbia, Burkina Faso, Poland, Denmark, Israel, the United Kingdom, and Djibouti (Kilpatrick et al. 2006). This method does not include the calculation of IBAs (import bird areas) as used in the Kilpatrick et al. study (2006). Also, this mapping technique would offers misleading visualization when there are only a few outbreaks caused by one spreading method in a large country (such as Russia), and depict the entire area as experiencing H5N1 by a certain method of spread. Nonetheless, there seems to be a trend of decreasing prevalence of spread via poultry trade, especially in 2011 (Figure 8.5). Since AIV testing is mostly used for flocks of poultry, not individual birds, testing and curing or culling wild migrating birds may be less successful and therefore may explain the continued spread of H5N1 through this pathway (Swayne and Spackman 2013). Also, a survey from 2002 to 2010 to OIE Delegates for countries with HPAI outbreaks, indicated that the lack of adequate resources for vaccination and the high cost of vaccines were among the top five most reported responses for why countries have not applied vaccines (Swayne and Spackman 2013). The economic status of European countries may have provided them the means to prevent new introductions by using expensive methods such as testing and vaccinations.

8.4 CONCLUSION

This study has examined the spatial and temporal dynamics of H5N1 outbreaks with various mapping techniques in order to determine the role of global trading and bird migration processes in H5N1 outbreaks from 2007 to 2011. The rate of spread analysis (Figure 8.3) determined that during EW1, there was a greater occurrence of outbreaks within a small spatial scale. Incongruously, the nearest neighbor function (Table 8.2), results show that EW4 had the greatest amount of local outbreaks and was the most clustered. The most likely method of spread (wild, poultry, or wild then poultry) for each outbreak was determined and mapped by country. After identifying four EWs throughout the study period, the potential pathways of H5N1 spread were mapped and several isolated outbreak clusters were identified as likely not being facilitated by bird migration. Both of these two methods (Figure 8.4 and Figure 8.5) showed that that spread by poultry trade has become less prevalent from 2007 to 2011 and from EW1 to EW4.

There are many limitations to large scale mapping of H5N1 influenza spread. In particular, a major limitation of the methods used in this study was that the final mapping model was based on spatiotemporal characteristics between outbreaks but did not include individual outbreak characteristics such as number of cases and types of bird species. Future studies should also consider how one can effectively map

multiple pathways simultaneously. Since this model mapped clusters chronologically, it misrepresented the movement of H5N1 when in reality, the influenza was moving in different areas of the world at the same time. It remains a challenge to map spread when considering the geometry of continent shapes such that bird migration is limited by separation of areas by the ocean and that multiple methods of bird movement must be considered. It is imperative to continue research and improve upon current models because understanding the spatiotemporal characteristics of H5N1spread is the first step in predication and mitigation techniques. Especially given the severity of H5N1 as a global health concern, there is a need for innovative mapping techniques for disease spread.

ACKNOWLEDGMENT

This research was initially supported by a Grant (Number PIV-005) awarded to Dongmei Chen from the Geomatics for Information Decision (GEOIDE), National Centre of Excellence, Canada. The authors would like to thank Masroor Hussain at the Department of Geography, Queen's University for help in developing the SRQRT tool.

REFERENCES

Capu I. and Alexander D. (2010). Perspectivies on the global threat: the challenge of avian influenza viruses for the world's veterinary community. *Avian Diseases*, 54:176–178.

Gilbert M., Xiao X., Domenech J., Martin V., Slingenbergh J. (2006). Anatidae migration in the western Palearctic and spread of highly pathogenic avian influenza H5N1 virus. *Emerging Infectious Diseases*, 12:1650–1656.

Kilpatrick A., Chmura A., Gibbons D., Flelscher R., Marra P., and Daszal P. (2006). Predicting the global spread of H5N1 avian influenza. *Proceedings of the National Academy of Sciences of the United States of America*, 103: 19368–19373.

Liu J., Xiaxo H., Lei F., Zhu Q., Qin K., Zhang X., Zhao D., Wang G., Feng Y., Ma J., Liu W., Wang J., and Gao G. F. (2005). Highly pathogenic H5N1 influenza virus infection in migratory birds. *Science* 309:1206.

Oyana T. J., Da D., and Scott K. E. (2006). Spatiotemporal distributions of reported cases of the avian influenza H5N1 (bird flu) in southern China in early 2004. *Avian Diseases*, 50:508–515.

Saito R., Paget J., Hitaka S., Sakai T., Sasaki A., van der Velde K., and Suzuki H. (2005). Geographic mapping method shows potential for mapping influenza activity in Europe. *Eurosurveillance*, 10(43), Article Id: 2824.

Si Y., de Boer W. F., and Gong P. (2013). Different environmental drivers of highly pathogenic avian influenza H5N1 outbreaks in poultry and wild birds. *PLoS One*, 8(1): e53362. DOI:10.1371/journal.pone.0053362.

Skog L., Hauska H., and Linde A. (2008). The Russian influenza in Sweden in 1889-90: an example of Geographic Information System analysis. *Eurosurveillance*, 13(49):1–7.

Swayne D. E. and Spackman, E. (2013). Current status and future needs in diagnostics and vaccines for high pathogenicity avian influenza. *Developments in Biologicals*. 135:79–94.

Toma B., Vaillancourt J. P., Dufour B., Eloit M., Moutou F., Marsh W., Benet J. J., Sanaa M., and Michel P. (1999). *Dictionary of Veterinary Epidemiology*. Ames, IA: Iowa State University Press.

U.S. Geological Survey [USGS]. (2013). Migration of Birds: Flight Speed and Rate of Migration. Available at http://www.npwrc.usgs.gov/resource/birds/migratio/speed.htm (accessed April 24, 2014).

Wallace R. G., Hodac H., Lathroc R. H., and Fitch W. M. (2007). A statistical phylogeography of influenza A H5N1. *Proceedings of the National Academy of Sciences of the United States of America*, 104:4473–4478.

World Health Organization. (2013). Avian Influenza. Available at http://www.who.int/mediacentre/factsheets/avian_influenza/en/ (accessed July 9, 2013).

Zhang Z. J., Chen D. M., Chen Y., Liu W. B., Wang W., Zhao F., and Yao B. (2010). Spatiotemporal data comparisons for global highly pathogenic avian influenza (HPAI) H5N1 outbreaks. *PLoS One*, 5:e15314.

Zhang Z., Chen D., Ward M. P., and Jiang Q. (2012). Transmissibility of the highly pathogenic avian influenza virus, subtype H5N1 in domestic poultry: a spatio-temporal estimation at the global scale. *Geospatial Health*, 7(1):135–143.